Magmatic eruptions and iron volatility in deep-sea hydrothermal fluids

Nicholas J. Pester*, Kang Ding, and William E. Seyfried, Jr.
Department of Earth Sciences, University of Minnesota, Minneapolis, Minnesota 55455, USA

ABSTRACT

During periods of volcanic activity, hydrothermal fluid chemistry changes drastically, becoming unusually dilute due to enhanced degrees of phase separation. Despite decreases in nearly all other metals, these dilute fluids maintain surprisingly high dissolved Fe concentrations. This is demonstrated by a 17 yr time series from 9°50′N on the East Pacific Rise, where two eruption cycles are separated by a decade of steady-state chemical and physical conditions. We report experimental data confirming a sharp increase in Fe solubility in low-salinity and low-density vapors that constitutes a reversal in behavior exhibited in near-critical vapors characteristic of the steady-state condition. In accordance with field observations during the eruptions, a fundamental divergence between the otherwise similar behaviors of Fe and Mn also results. This helps explain how Fe fluxes are maintained during magmatic events, which may have important implications for the succession and temporal evolution of vent-related fauna. Calibrated geochemical proxies for subseafloor reaction conditions (pressure-temperature) now allow us to elucidate hydrothermal processes from steady state through eruptive and recovery stages at the 9°50′N system.

INTRODUCTION

Subseafloor magma chambers associated with mid-ocean ridge spreading centers provide a persistent and robust heat source that fuels seawater convection, facilitating chemical exchange with newly formed oceanic crust (Kent et al., 1993; Wilcock et al., 2009). Seawater is thus transformed into "black smoker" hydrothermal fluids enriched in both reduced gases (H_2, H_2S) and transition metals (Fe, Mn, Zn, and Cu). The chemical composition of fluids venting at the seafloor can remain stable (steady state) on decadal time scales (e.g., Pester et al., 2012; Von Damm, 2004), producing a noteworthy flux to the world's oceans, while also forming seafloor massive sulfide deposits (Coogan and Dosso, 2012; Hannington et al., 2011; Saito et al., 2013). Oxidation of dissolved Fe, H_2, and H_2S fuels microbial metabolism, providing the basal energy critical to the unique ecological niche associated with deep-sea vents (Jannasch and Mottl, 1985; Orcutt et al., 2011; Shank et al., 1998).

Experimental and field studies of marine hydrothermal systems indicate that both heterogeneous (fluid-mineral) equilibria and homogeneous (fluid) phase separation dictate the chemical evolution of vent fluids (Bischoff and Rosenbauer, 1987; Butterfield et al., 1997; Pester et al., 2012; Seyfried et al., 1991; Von Damm, 2004). Fluid-mineral exchange reactions buffer pH and redox, effectively leaving only chloride to charge-balance cations in solution. Thus, chlorinity constrains the carrying capacity of most dissolved metals. Because Cl is conservative during mineral alteration, persistent observations of chloride variability in vent fluids (relative to seawater) indicate the routine occurrence of subseafloor phase separation, even under steady-state chemical and physical conditions. Intersection of the two-phase boundary (essentially the critical curve of an electrolyte solution) results in the coexistence of a lower-chlorinity vapor and a higher-chlorinity liquid (Driesner and Heinrich, 2007, and references therein). The contrasting density of these fluids facilitates segregation by buoyancy-driven ascent of the vapor. Fluids moderately depleted in chloride are characteristic of steady state, maintained by a balance between a stable heat flux from the magma chamber and the heat-capacity/expansivity maxima of near-critical fluids (Jupp and Schultz, 2000). Steady state is periodically perturbed by magmatic intrusions and eruptions, resulting in fluids with unusually low chlorinity and high H_2 and H_2S contents (Butterfield et al., 1997; Lilley et al., 2003; Von Damm, 2000; Von Damm and Lilley, 2004). This is exemplified by a comprehensive time-series data set of fluid chemistry from two vent structures (P vent and Bio 9) at 9°50′N on the East Pacific Rise (EPR). These data show dramatic departures from steady state (ca. 1996–2004) associated with two eruptive cycles (1991–92 and 2005–2006; Fig. 1; Fig. DR1 in the GSA Data Repository[1]). Higher temperature (T) and/or lower pressure (P) within the two-phase region results in lower-chlorinity vapors (and higher-chlorinity liquids), which is consistent with magmatic intrusion into more shallow crust.

Fe and Mn compose >95% of the transition metal inventory of deep-sea vent fluids, and the solubility of each metal is similarly affected by pH and T (~300 °C to 450 °C) during hydrothermal alteration of basalt (Pester et al., 2011; Seyfried et al., 1991; Seyfried and Janecky, 1985). Consequently, the Fe/Mn ratio of a fluid can be used to estimate T at the time of last equilibration (T_{eq}) with subseafloor minerals (Pester et al., 2011, 2012) for both the steady-state and recovery stages of the EPR 9°50′N time series (Fig. 1D). However, fluids affected by the eruptions have substantially higher Fe/Mn ratios than those at steady state, and we note that these data exhibit decreases in the Mn/Cl ratios with concomitant increases in the Fe/Cl ratios (Fig. 1). This casts doubt on the otherwise intuitive notion that the higher Fe/Mn ratios reflect higher T_{eq} because this should effect an increase in the chloride ratio of both metals.

Recent experimental data (Foustoukos and Seyfried, 2007a) demonstrate that phase separation induced by isothermal decompression can evolve vapors with Fe/Cl ratios at least twice as high as those of the single-phase fluid in a buffered system containing pyrite-pyrrhotite-magnetite (PPM) (Fig. DR1B). PPM is likely analogous to the steady-state redox buffer in EPR hydrothermal systems (Seyfried et al., 1991), and the experimental vapor data also show increases in H_2 and H_2S consistent with those observed during the EPR 9°50′N eruptions (Fig. DR1). This means temperatures higher than steady-state and/or a shift in redox control are not necessarily required to interpret the changes in vent fluid chemistry. However, an explanation for the divergent behavior of Fe and Mn is imperative. For example, the likelihood that Mn was rock-limited through the eruptive stages is low because the fluid Mn/Cl ratios were not universally attenuated relative to steady state.

EXPERIMENTAL RESULTS

While enhanced gas solubility in lower-density vapor is perhaps intuitively clear, the same is decidedly not the case for Fe. We have therefore performed a series of hydrothermal flow experiments designed to assess the fractionation of dissolved Fe and Mn during phase separation at P-T conditions relevant to magmatically perturbed hydrothermal systems. The experiments were conducted in the absence of minerals to better understand the role of phase separation alone on the mass transport of Fe and Mn. Each experiment entailed monitoring the composition of vapors and liquids derived from a Fe- and Mn-bearing (NaCl-dominated)

*Current address: Earth Sciences Division, Lawrence Berkeley National Laboratory, Berkeley, California 94720, USA; E-mail: NJPester@lbl.gov.

[1]GSA Data Repository item 2014101, methods, Figures DR1–DR5, and Tables DR1–DR6, is available online at www.geosociety.org/pubs/ft2014.htm, or on request from editing@geosociety.org or Documents Secretary, GSA, P.O. Box 9140, Boulder, CO 80301, USA.

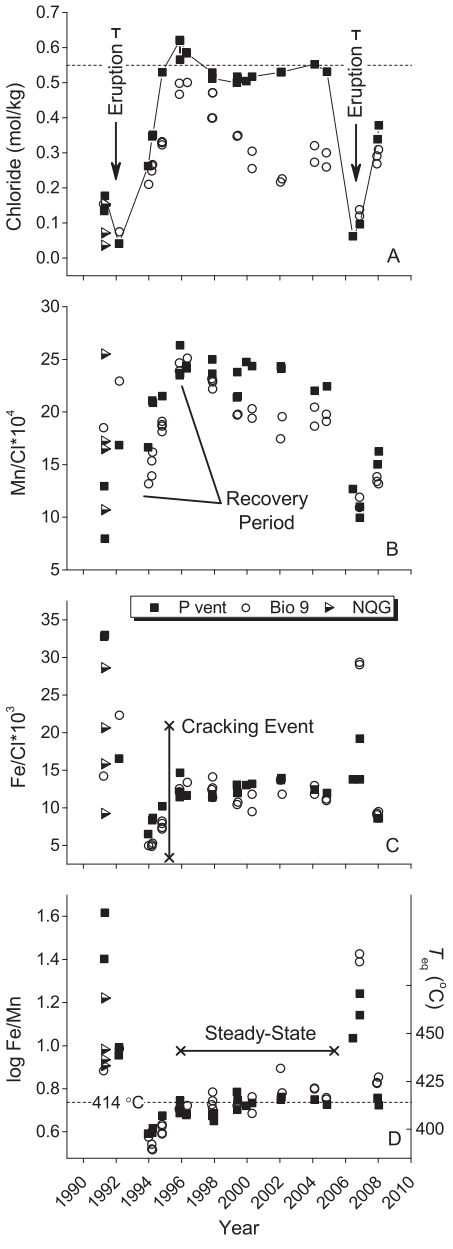

Figure 1. Time-series fluid chemistry (Bryce et al., 2011; Fornari et al., 2012; Von Damm, 2000, 2004; Table DR6 [see footnote 1]) from vent structures P vent and Bio 9 (including Bio 9′) as well as N, Q, and G vents (data only available for 1991) at East Pacific Rise, 9°50′N. A: Dissolved chloride (dashed line represents seawater; solid line connects P vent data to guide eye). B: Mn/Cl ratios. C: Fe/Cl ratios. D: Fe/Mn ratios. Right axis defines temperature at time of last equilibration (T_{eq}), calibrated to 450 °C (T_{eq} = 331.24 + 112.41*log [Fe/Mn]; Pester et al., 2011). Three general stages (eruption, recovery, and steady state) are indicated by fluid chemistry. After 1991–1992 eruptions, T_{eq} was as low as ~390 °C, increasing to average steady-state value of ~414 °C (ca. 1996–2004) following seismic cracking event in 1995 (Sohn et al., 1998). Most of the eruptive-stage data do not fall within calibration range of geothermometer. Time-series H_2 and H_2S, as well as raw Fe and Mn concentrations, are depicted in Figs. DR1A and DR5, respectively (see footnote 1).

source fluid, which was subjected to precisely controlled *P-T* conditions in a Ti hydrothermal reactor. Experimental methods and data are detailed in the Data Repository.

Given that charge balance must be maintained, the vapor-liquid partitioning of Fe and Mn can be demonstrated by a change in the metal/Cl (*M*/Cl) ratio with changing chlorinity. The experimental data indicate surprisingly large changes in vapor *M*/Cl ratios, whereas those of the coexisting liquids remain consistent with that of the bulk (single-phase) fluid due to mass-balance constraints (Fig. 2; Fig. DR3). Near-critical phase separation results in predictable (linear) decreases of vapor Fe/Cl and Mn/Cl ratios with chlorinity; and normalization of vapor compositions from separate experiments yields a unique and independent partition coefficient for each metal (Fig. 2; Fig. DR3). However, deviations from these linear relationships occur under more extreme conditions of phase separation (i.e., lower vapor densities), where the *M*/Cl ratios abruptly begin to increase with further decreases in chlorinity/density (Fig. 2; Fig. DR3). This is similar to previously reported vapor enrichment of mobile trace alkalis (Foustoukos and Seyfried, 2007b), and herein we use the term "volatility" to describe this phenomenon. For the transition metals, however, this constitutes an unexpected reversal in the partitioning behavior observed at conditions nearer the critical curve.

Mn volatility occurs only in the lowest chlorinity/density vapors. Phase separation and associated Fe volatility can therefore effect an order of magnitude increase in the Fe/Mn ratio, while simultaneously increasing and decreasing the Fe/Cl and Mn/Cl ratios, respectively (Fig. 2). Such phenomena are consistent with the systematic behavior of Fe-Mn-Cl observed in fluids associated with the EPR 9°50′N eruptions (Fig. 1). We note that the experimental volatility (i.e., a decrease in vapor chlorinity with a concurrent increase in the Fe/Cl ratio) demonstrates a fundamental increase in Fe solubility given the fixed Fe/Cl ratio of the coexisting liquid. At similar *P-T* conditions in a natural system, Fe-bearing minerals should respond to this enhanced solubility, resulting in additive increases in the Fe/Cl ratio of both vapors and liquids (e.g., Fig. DR1B). Such a mechanism appears necessary to explain the highest Fe/Cl ratios measured at EPR 9°50′N. In other words, phase separation of a fluid equivalent in composition to those measured throughout the steady-state period cannot alone fully account for the flux of Fe observed during the eruptions.

The surprisingly high vapor affinity of Fe is best explained as a tendency to form stronger complexes than other first-row transition metals (e.g., Irving and Williams, 1953). The vapor species of divalent transition metals is uncertain at the conditions of our experiments, but spectroscopic studies of higher-salinity/density liquids

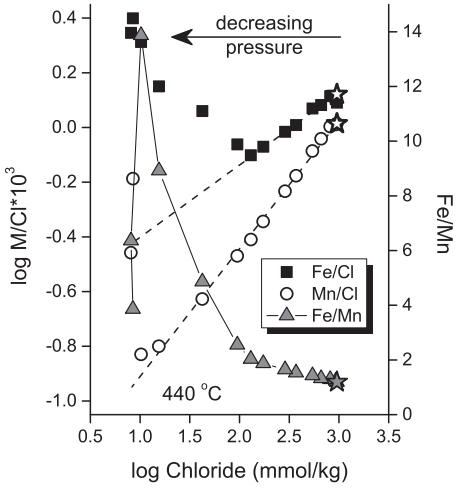

Figure 2. Vapor chemistry from experiment 5: Cl versus metal/Cl (*M*/Cl) ratio for Fe and Mn (left axis) and associated Fe/Mn ratios (right axis). Decreasing pressure (or increasing temperature) relative to critical point (star symbols) results in evolution of vapors with decreasing chlorinity/density. Both Fe and Mn initially exhibit decreasing vapor affinity with chlorinity that is predictable based on our combined experimental data (dashed lines: log [Fe/Cl] = 0.264*log Cl, and log [Mn/Cl] = 0.467*log Cl; see Fig. DR3 [see footnote 1] for derivation of partition coefficients). Fe exhibits volatility well before Mn, the latter requiring conditions at or near halite saturation.

(single-phase at similar temperatures) suggest the dominance of tetrahedral $[MCl_4]^{2-}$ as follows:

$$\left[MCl_2\left(OH_2\right)_2\right]^0 + 2\,NaCl^0 = 2\,Na^+ \cdot \left[MCl_4\right]^{2-} + 2\,H_2O, \quad (1)$$

and Na may be closely associated with any tetra- and tri-chloro complexes due to the favorability of neutral species in low-density hydrothermal fluids (Chen et al., 2005; Hoffmann et al., 1999). It is possible that volatility coincides with a leftward shift in Equation 1 due to the decreasing NaCl/H_2O ratio. For example, our data indicate Fe volatility occurs at *P-T* conditions where chlorinity is low enough that the vapor density approaches that of pure H_2O at the equivalent *P* and *T* (0.2–0.25 g/cm^3, Fig. DR4). This density range is sufficiently reproducible that a Fe volatility boundary may be estimated as a function of *P* and *T* within the vapor-liquid stability field. Assuming that volatility in part contributes to eruptive-stage Fe fluxes at EPR 9°50′N, this boundary can be used to better constrain prevailing subseafloor reaction conditions for these time periods (Fig. 3B).

DISCUSSION

Attempting to quantitatively decouple the effects of phase separation from fluid-mineral

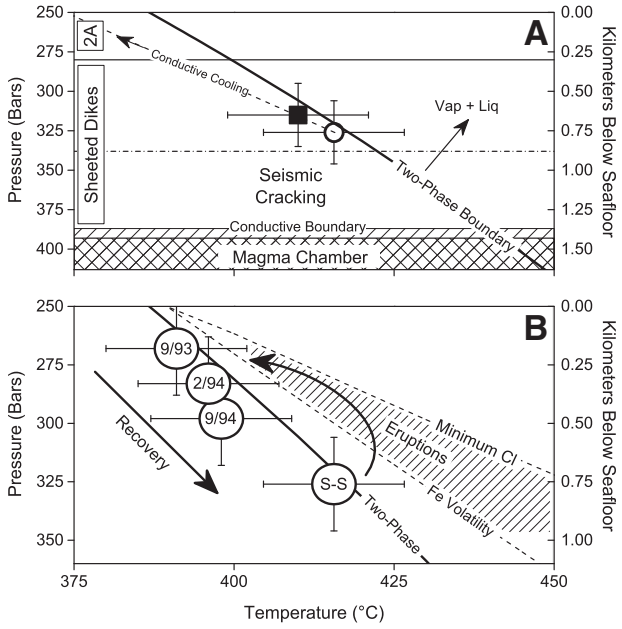

Figure 3. Schematic of geophysical (steady-state) and phase-equilibria constraints on pressure-temperature (*P-T*) of subseafloor hydrothermal processes at East Pacific Rise, 9°50′N. A: Steady-state conditions. Magma chamber, located ~1.43 km below seafloor, is overlain by ~1 km of sheeted dikes followed by ~0.3 km of extrusive basalt (layer 2A) (Harding et al., 1993; Kent et al., 1993). Steady-state *P-T* of last equilibration, based on Fe/Mn and Si (Pester et al., 2011), is shown for Bio 9 (open circle) and P vent (square). Quartz solubility was calculated by substituting NaCl solution densities after Driesner and Heinrich (2007) into equation of Von Damm et al. (1991), which agrees well with ongoing calibration experiments conducted at near-critical conditions in our lab. *P-T* conditions for Bio 9 and P vent independently coincide with (NaCl-H_2O) two-phase boundary/critical curve (region to right is that of vapor-liquid coexistence [Vap + Liq]). Steady-state depths lie just above a region of persistent seismic activity due to fluid penetration into hot rock, though broad-scale circulation may be more limited (Sohn et al., 1998; Tolstoy et al., 2008). Possible conductive cooling trend is shown for reference. For example, average temperature at time of last equilibration (T_{eq}) for P vent and Bio 9 is ~414 °C (see also Fig. 1D), and average exit *T* (measured at the seafloor) is ~373 °C. B: Model of time-series cycle from steady state through eruption and recovery for Bio 9 vent (geophysical constraints are omitted, note shallower depth scale). Dates (month/year) are given inside recovery stage data points. S-S—steady state. All error bars represent 95% prediction limit. Volatility boundary of Fe is estimated as an isopycnal (0.23 g/cm³) based on experimental data (Fig. DR4 [see footnote 1]). *P-T* associated with eruptions should fall between this boundary and the isopleth of minimum chloride measured in vent fluids (30 mmol/kg). Please see text for further discussion.

equilibria in natural hydrothermal systems carries some uncertainty because *P* and *T* affect both processes, which, furthermore, occur at different rates (the former being more rapid). Nonetheless, we have sufficient evidence to schematically reconstruct the *P-T* of subseafloor hydrothermal reactions throughout the three indicated stages (eruption/magmatism, recovery, and steady state) in the EPR 9°50′N time series (Figs. 1 and 3). Our experimental data demonstrate that near-critical phase separation results in minimal Fe/Mn fractionation and that it is predictable. Thus, the fluid chemistry from the steady-state and eruption recovery periods falls within the calibration field of the Fe/Mn geothermometer (Pester et al., 2011) (Fig. 1D). Calculated temperatures (T_{eq}), combined with constraints imposed by quartz solubility (Pester et al., 2011, 2012; Von Damm et al., 1991), suggest that reaction conditions in open systems are usually limited by the fluid's critical curve (likely due to the aforementioned heat-capacity/expansivity maxima). During magmatic events, however, reactions deeper within the two-phase region are indicated (Fig. 3B).

The combined geochemical and geophysical evidence is consistent with a general cycle in which localized magmatic intrusions dramatically perturb the established hydrothermal system, driving deeper (hot) crustal fluids to shallower depths. Intrusions and eruptions can result in the destruction of established vent sites and associated biology (though apparently not the case for P vent and Bio 9) as well as contribute to the emergence of new sites (Fornari et al., 2012; Shank et al., 1998). Relative to steady state, a temporarily shallower heat source means that fluids, as part of the recovery stage, will then intersect the two-phase boundary (critical curve) at lower *P-T*. Hydrothermal circulation systematically causes the heat source to deepen, allowing reaction temperatures to increase in accordance with the critical curve (Fig. 3B). Ultimately, heat- and mass-transfer processes attain steady state under constraints imposed by the underlying magma chamber. Interestingly, the return to steady state at EPR 9°50′N following the 1991–1992 eruptions coincided with a seismic cracking event recorded in 1995 (Sohn et al., 1998) (Fig. 1). Furthermore, the inferred crustal location of the source for steady-state vent fluids is broadly consistent with transition to a zone of persistent micro-seismicity within the lower sheeted dike complex (Sohn et al., 1998; Tolstoy et al., 2008) (Fig. 3A). The time series indicates ~3 yr is required for the system to return to steady state following a major magmatic event (Fig. 1; Fig. DR1A), though the physical mechanism accounting for the evolution of hydrothermal heat extraction on such a time scale is uncertain. The low-chlorinity vapors associated with the eruptive stages appear relatively short lived, yet the enhanced flux of H_2 and H_2S (Lilley et al., 2003; Von Damm and Lilley, 2004), in addition to that of Fe discussed herein, may aid in establishing a sufficient foundation for nascent ecosystems (Shank et al., 1998) in the wake of mature biological communities destroyed during the eruptions.

ACKNOWLEDGMENTS

We thank the captain and crew of R/V *Atlantis*, the Alvin Group, and D. Foustoukos for assistance in acquiring the EPR 9-10°N fluid samples, as well as R. Knurr for analyses of both the field and experimental samples. We also thank J. Bryce and F. Prado for making available the unpublished fluid chemical data from EPR 9-10°N acquired between 2002 and 2007 (http://dx.doi.org/10.1594/IEDA/100031). Reviews by David Butterfield and Laurence Coogan improved the clarity and content of the manuscript. Financial support for this research was provided by National Science Foundation grants 0927615, 0751771, 0813861 (WES, KD).

REFERENCES CITED

Bischoff, J.L., and Rosenbauer, R.J., 1987, Phase separation in seafloor geothermal systems: An experimental study on the effects of metal transport: American Journal of Science, v. 287, p. 953–978, doi:10.2475/ajs.287.10.953.

Bryce, J., Prado, F., and Von Damm, K., 2011, Marine Geoscience Data System: http://www.marine-geo.org, doi:10.1594/IEDA/100031 (accessed March 2012).

Butterfield, D.A., Jonasson, I.R., Massoth, G.J., Feely, R.A., Roe, K.K., Embley, R.E., Holden, J.F., McDuff, R.E., Lilley, M.D., and Delaney, J.R., 1997, Seafloor eruptions and evolution of hydrothermal fluid chemistry: Philosophical Transactions of the Royal Society of London A, v. 355, p. 369–386.

Chen, Y., Fulton, J.L., and Partenheimer, W., 2005, The structure of the homogenous oxidation catalyst, $Mn(II)(Br^{-1})_x$, in supercritical water: An X-ray absorption fine-structure study: Journal of the American Chemical Society, v. 127, p. 14,085–14,093, doi:10.1021/ja053421v.

Coogan, L.A., and Dosso, S., 2012, An internally consistent, probabilistic, determination of ridge-axis hydrothermal fluxes from basalt-hosted hydrothermal systems: Earth and Planetary Science Letters, v. 323–324, p. 92–101, doi:10.1016/j.epsl.2012.01.017.

Driesner, T., and Heinrich, C.A., 2007, The system H_2O-NaCl. Part I: Correlation formulae for phase relations in temperature-pressure-composition space from 0 to 1000°C, 0 to 5000 bar, and 0 to 1 X_{NaCl}: Geochimica et Cosmochimica Acta, v. 71, p. 4880–4901, doi:10.1016/j.gca.2006.01.033.

Fornari, D.J., and 16 others, 2012, The East Pacific Rise between 9°N and 10°N: Twenty-five years of integrated, multidisciplinary oceanic spreading center studies: Oceanography (Washington, D.C.), v. 25, p. 18–43, doi:10.5670/oceanog.2012.02.

Foustoukos, D.I., and Seyfried, W.E., Jr., 2007a, Fluid phase separation processes in submarine hydrothermal systems, *in* Liebscher, A., and Heinrich, C.A., eds., Fluid–fluid interactions: Reviews in Mineralogy Geochemistry, v. 65, p. 213–239.

Foustoukos, D.I., and Seyfried, W.E., Jr., 2007b, Trace element partitioning between vapor, brine and halite under extreme phase separation conditions: Geochimica et Cosmochimica Acta, v. 71, p. 2056–2071, doi:10.1016/j.gca.2007.01.024.

Hannington, M., Jamieson, J., Monecke, T., Petersen, S., and Beaulieu, S., 2011, The abundance of seafloor massive sulfide deposits: Geology, v. 39, p. 1155–1158, doi:10.1130/G32468.1.

Harding, A.J., Kent, G.M., and Orcutt, J.A., 1993, A multichannel seismic investigation of the upper crustal structure at 9°N on the East Pacific Rise: Implications for crustal accretion: Journal of Geophysical Research, v. 98, p. 13,925–13,944, doi:10.1029/93JB00886.

Hoffmann, M.M., Darab, J.G., Palmer, B.J., and Fulton, J.L., 1999, A transition in the Ni^{2+} complex structure from six- to four-coordinate upon formation of ion pair species in supercritical water: An X-ray absorption fine structure, near-infrared, and molecular dynamics study: The Journal of Physical Chemistry A, v. 103, p. 8471–8482, doi:10.1021/jp990435c.

Irving, H., and Williams, R.J.P., 1953, The stability of transition-metal complexes: Journal of the Chemical Society, p. 3192–3210, doi:10.1039/jr9530003192.

Jannasch, H.W., and Mottl, M.J., 1985, Geomicrobiology of deep-sea hydrothermal vents: Science, v. 229, p. 717–725, doi:10.1126/science.229.4715.717.

Jupp, T., and Schultz, A., 2000, A thermodynamic explanation for black smoker temperatures: Nature, v. 403, p. 880–883, doi:10.1038/35002552.

Kent, G.M., Harding, A.J., and Orcutt, J.A., 1993, Distribution of magma beneath the East Pacific Rise between the Clipperton Transform and the 9°17′N Deval from forward modeling of common depth point data: Journal of Geophysical Research, v. 98, p. 13,945–13,969, doi:10.1029/93JB00705.

Lilley, M.D., Lupton, J.E., Butterfield, D.A., and Olson, E., 2003, Magmatic events can produce rapid changes in hydrothermal vent chemistry: Nature, v. 422, p. 878–881, doi:10.1038/nature01569.

Orcutt, B.N., Sylvan, J.B., Knab, N.J., and Edwards, K.J., 2011, Microbial ecology of the dark ocean above, at, and below the seafloor: Microbiology and Molecular Biology Reviews, v. 75, p. 361–422, doi:10.1128/MMBR.00039-10.

Pester, N.J., Rough, M., Ding, K., and Seyfried, W.E., Jr., 2011, A new Fe/Mn geothermometer for hydrothermal systems: Implications for high-salinity fluids at 13°N on the East Pacific Rise: Geochimica et Cosmochimica Acta, v. 75, p. 7881–7892, doi:10.1016/j.gca.2011.08.043.

Pester, N.J., Reeves, E.P., Rough, M.E., Ding, K., Seewald, J.S., and Seyfried, W.E., Jr., 2012, Subseafloor phase equilibria in high-temperature hydrothermal fluids of the Lucky Strike Seamount (Mid-Atlantic Ridge, 37°17′N): Geochimica et Cosmochimica Acta, v. 90, p. 303–322, doi:10.1016/j.gca.2012.05.018.

Saito, M.A., Noble, A.E., Tagliabue, A., Goepfert, T.J., Lamborg, C.H., and Jenkins, W.L., 2013, Slow-spreading submarine ridges in the South Atlantic as a significant oceanic iron source: Nature Geoscience, v. 6, p. 775–779, doi:10.1038/ngeo1893.

Seyfried, W.E., Jr., and Janecky, D.R., 1985, Heavy metal and sulfur transport during subcritical and supercritical hydrothermal alteration of basalt: Influence of fluid pressure and basalt composition and crystallinity: Geochimica et Cosmochimica Acta, v. 49, p. 2545–2560, doi:10.1016/0016-7037(85)90123-1.

Seyfried, W.E., Jr., Ding, K., and Berndt, M.E., 1991, Phase equilibria constraints on the chemistry of hot spring fluids at mid-ocean ridges: Geochimica et Cosmochimica Acta, v. 55, p. 3559–3580, doi:10.1016/0016-7037(91)90056-B.

Shank, T., Fornari, D., Von Damm, K.L., Lilley, M., Haymon, R., and Lutz, R.A., 1998, Temporal and spatial patterns of biological community development at nascent deep-sea hydrothermal vents (9°50′N, East Pacific Rise): Deep-sea Research, Part II: Topical Studies in Oceanography, v. 45, p. 465–515, doi:10.1016/S0967-0645(97)00089-1.

Sohn, R.A., Fornari, D.J., Von Damm, K.L., Hildebrand, J.A., and Webb, S.C., 1998, Seismic and hydrothermal evidence for a cracking event on the East Pacific Rise crest at 9°50′N: Nature, v. 396, p. 159–161, doi:10.1038/24146.

Tolstoy, M., Waldhauser, F., Bohnenstiehl, D.R., Weekly, R.T., and Kim, W.Y., 2008, Seismic identification of along-axis hydrothermal flow on the East Pacific Rise: Nature, v. 451, p. 181–184, doi:10.1038/nature06424.

Von Damm, K.L., 2000, Chemistry of hydrothermal vent fluids from 9°–10°N, East Pacific Rise: "Time zero," the immediate posteruptive period: Journal of Geophysical Research, v. 105, p. 11,203–11,222, doi:10.1029/1999JB900414.

Von Damm, K.L., 2004, Evolution of the hydrothermal system at East Pacific Rise 9°50′N: Geochemical evidence for changes in the upper oceanic crust, *in* German, C.R., et al., eds., Mid-ocean ridges: Hydrothermal interactions between the lithosphere and oceans: American Geophysical Union Geophysical Monograph 148, p. 285–305.

Von Damm, K.L., and Lilley, M.D., 2004, Diffuse flow hydrothermal fluids from 9°50′N East Pacific Rise: Origin, evolution and biogeochemical controls, *in* Wilcock, W.S., et al., eds., The subseafloor biosphere at mid-ocean ridges: American Geophysical Union Geophysical Monograph 144, p. 245–268.

Von Damm, K.L., Bischoff, J.L., and Rosenbauer, R.J., 1991, Quartz solubility in hydrothermal seawater: An experimental study and equation describing quartz solubility for up to 0.5 M NaCl solutions: American Journal of Science, v. 291, p. 977–1007, doi:10.2475/ajs.291.10.977.

Wilcock, W.S.D., Hooft, E.E.E., Toomey, D.R., McGill, P.R., Barclay, A.H., Stakes, D.S., and Ramirez, T.M., 2009, The role of magma injection in localizing black-smoker activity: Nature Geoscience, v. 2, p. 509–513, doi:10.1038/ngeo550.

Manuscript received 30 August 2013
Revised manuscript received 6 December 2013
Manuscript accepted 12 December 2013

Printed in USA